第 31 卷第 3 期
2015 年 3 月

无 机 化 学 学 报
CHINESE JOURNAL OF INORGANIC CHEMISTRY

Vol.31 No.3
619-626

类似花状结构介晶钴的大规模控制合成及磁性能

关明云[1,2] 简 妍[1] 孙建华[1,2] 徐 正*,[2]

([1]江苏理工学院化学与环境工程学院,江苏省贵金属深加工及应用重点建设实验室,常州 213001)

([2]南京大学化学与化工学院,配位化学国家重点实验室,南京 210093)

摘要:以二乙烯三胺(DETA)作为配位剂,快速合成了纳米粒子定向组装构成的类似花状的介晶钴。通过控制反应的速率和配位剂的种类,依次获得了精美的钴花、差形貌的枝晶、由纳米粒子或纳米片构成的微球。配位剂在介晶钴的形成过程中起了很重要的作用。探讨了介晶钴花的形成机理。介晶钴不但具有钴纳米晶的性能(在 300 K 时矫顽力 260 Oe),而且拥有块体钴的性能(饱和磁化强度 168 emu·g^{-1})。合成方法简便、有效且具有较高的产率。

关键词:钴;晶体组装;介晶;取向搭接

中图分类号:TQ050.4 **文献标识码**:A **文章编号**:1001-4861(2015)03-0619-08

DOI:10.11862/CJIC.2015.084

Flower-Like Mesocrystal Cobalt: Controllable Synthesis in Large Scale and Magnetic Property

GUAN Ming-Yun[1,2] JIAN Yan[1] SUN Jian-Hua[1,2] XU Zheng*,[2]

([1]*Jiangsu Key Laboratory of Precious Metals Chemistry, School of Chemistry and Environmental Engineering, Jiangsu University of Technology, Changzhou, Jiangsu* 213001, *China*)

([2]*State Key Laboratory of Coordination Chemistry, School of Chemistry and Chemical Engineering, Nanjing University, Nanjing* 210093, *China*)

Abstract: Using diethylenetriamine (DETA) as coordination agent, a well-defined flower-like cobalt mesocrystal was synthesized rapidly by nanoparticles self assembly in oriented fashion. By adjusting reaction rate and kind of coordination agents, morphologies of cobalt can be transformed from nice-look flower, via poor-look dendrite, to microsphere composed of nanoparticles or nanoplates. DETA plays an important role in the formation process of cobalt mesocrystal. The possible formation mechanism is proposed. The cobalt mesocrystals not only exhibit Co nanocrystals property (an enhanced coercive force being 260 Oe at 300 K), but also have bulk Co property (saturation magnetization being 168 emu·g^{-1}). The synthesis method in large scale is facile and effective with high yield.

Key words: cobalt; crystallization assembly; mesocrystal; oriented attachment

Mesocrystals defined by Cölfen et al.[1-3] have attracted great attention for potentially exciting applications, such as biominerals and their minetics, functional ceramics, sensors, lithium-ion battery, and

收稿日期:2014-11-03。收修改稿日期:2014-12-23。

国家 973 重点建设项目基础研究项目(No.2007CB936302),国家自然科学基金-面上项目(No.21373103),江苏省自然科学基金-面上项目(No.BK2011260)资助项目。

*通讯联系人。E-mail:zhengxu@nju.edu.cn

photovoltaic devices etc. In contrast to ion-mediated classical growth mechanism of a single crystal, the mesocrystals are constructed by nanocrystals instead of atoms/molecules as building blocks in oriented-attachment fashion. They not only have the properties from the nanocrystals but also display collective properties produced by their interaction[4]. Further intensive study on formation mechanism of mesocrystals is helpful for constructing novel materials by bottom-up approaches. The number of reports on mesocrystals rapidly increases[5-25], but the types of mesocrystals are quite limited, such as carbonate[1,19], metal oxide[11], copper oxalate[15], Ag[22] etc. It is urgent to explore a facile method to extend the spectrum of the mesocrystals.

As one of the important magnetic metal materials, cobalt has been the focus of intensive research owing to their physical properties and technological applications: such as high-density data storage, medical diagnosis, and bio-separation[26-29]. Various morphologies, such as nanoparticle, nanorod, nanotube, dendrite and snowflake microcrystal, have been synthesized[26-32]. Here, we report a facile synthesis method in large scale for well-defined 3D flower-like cobalt mesocrystals. The time for Co mesocrystal formation is very short, only ~10 min. The formation mechanism is investigated carefully. In addition, nice-look flowers, poor-look dendrite, microsphere composed of Co nanoparticles or nanoplates are obtained by simply adjusting reduction rate of Co^{2+}.

1 Experimental

Cobalt chloride($CoCl_2$), diethylenetriamine(DETA), ethylenediamine(EN), sodium hydroxide(NaOH), and diamine hydrate($N_2H_4\cdot H_2O$) were purchased from the Sinopharm Chemical Reagent Company. All chemical reagents were of analytical grade and were used without further purification.

1.1 Synthesis

2.5 mL $CoCl_2$ aqueous solution (1.429 $mol\cdot L^{-1}$) were mixed with 7.5 mL DETA under stirring, 10 mL of NaOH aqueous solution (5 $mol\cdot L^{-1}$) and 5 mL of $N_2H_4\cdot H_2O$ (85%) were added into the above solution under stirring for 1 min. The resultant solution was transferred into autoclave, and maintained at 100 ℃ for 10 min. The black precipitates at the bottom were collected and washed with absolute ethanol and then dried in a vacuum oven at 80 ℃.

1.2 Characterizations

Products were characterized by X-ray powder diffraction (XRD) (Shimadzu XD-3A X-ray diffractometer with Ni filter, Cu $K\alpha$ radiation (λ=0.154 18 nm) accelerating voltage of 40 kV, emission current 20 mA, scanning range 30°~80°, scanning rate of 0.06°·s^{-1}). The transmission electron microscopy (TEM) images, high-resolution TEM (HRTEM) images and selected-area electron diffraction (SAED) patterns were obtained on a FEI Tecnai G^2 20 S-TWIN high-resolution transmission electron microscope, using an accelerating voltage of 200 kV. Scanning electron microscopy (SEM) images were taken with a JEOL JSM 5610LV apparatus with an accelerating voltage of 15 kV. Magnetization measurements of the products were performed on a superconducting quantum interference device(SQUID) magnetometer (MPMS XL-7 Quantum Design). Zero-field-cooling (ZFC) and field-cooling (FC) curves were recorded under 100 Oe applied field between 575 K and 750 K.

2 Results and discussion

2.1 Morphology and structure characterization

The low-magnification SEM images (Fig.1a) clearly reveal the three-dimensional (3D) feature of the Co flower-like structure. The high-magnification SEM and field emission SEM (FESEM) images in Fig. 1b, c respectively show perfect flower-like structure and snowflake structure composed of several petals with a thick main trunk and many secondary trunks on both sides of the main trunk. The surface of the petals is not flat with many grooves, which is not expected for a single crystal. The length of the main trunks and the secondary branches are 2~8 μm and 0.1~2.6 μm respectively. The thickness of the petals is about several hundred nanometers. The XRD pattern of the products (Fig.1d) indicates that all the diffraction peaks are indexed to the hexagonal phase

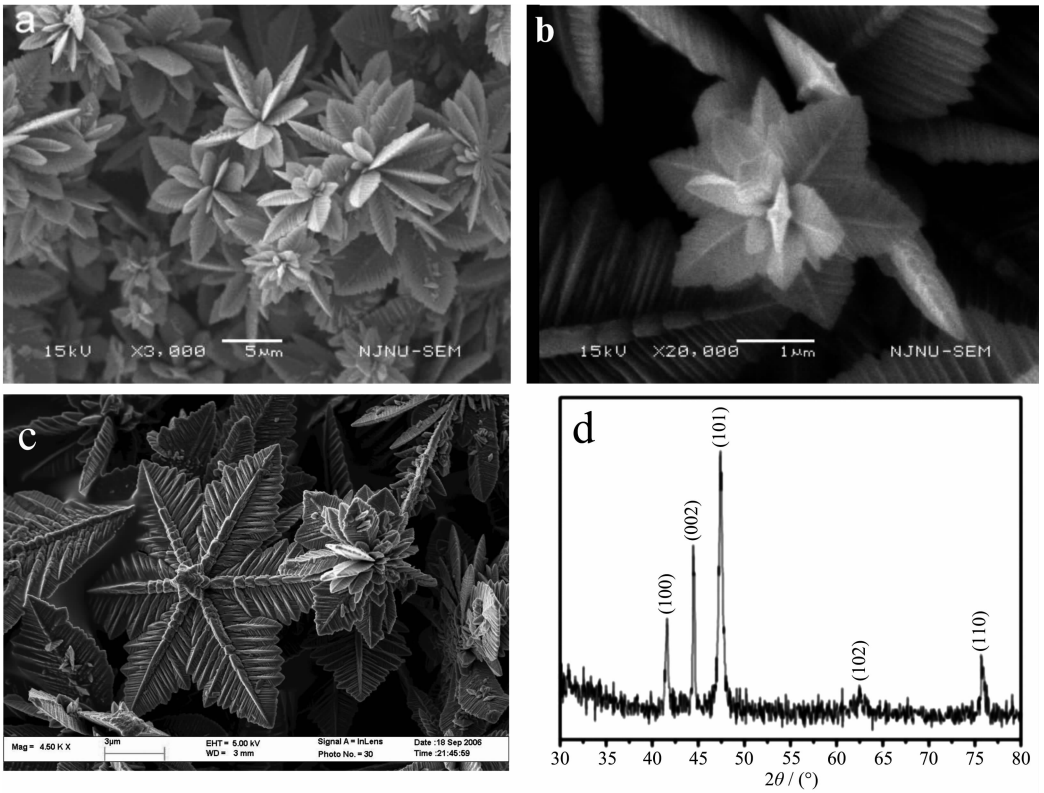

Fig.1　(a) Low-magnification SEM image of Co flower-like mesocrystals, (b) High-magnification SEM images of 3D Co flower-like mesocrystals, (c) FESEM images of Co snowflake mesocrystals, (d) XRD pattern of Co flower-like mesocrystals

of Co (PDF No.05-0727) in good agreement with the literature reports [31-32]. No other impurity phase is detected. The energy-dispersive X-ray spectroscopy (EDS) analysis of the product (supporting information (SI)-1) shows that the sample is essentially pure cobalt which is consistent with the XRD results. The small amount of oxygen might attribute to the absorption oxygen or the oxidation of the Co surface partly.

TEM images in SI-2a, b further reveal a well-defined flower-like structure with a thick main trunk and highly ordered second and third generation trunk. After closer look at the FESEM image of Fig.2a, we can clearly see that the main trunk, the second and third generation trunk are composed of many spines. Dark field TEM image of Co petal in Fig.2b also shows that the petal is composed of nanoparticles. It seems like polycrystalline. Fig.2c shows the TEM image of a Co petal. The three parts of HRTEM images marked as A, B and C in Fig.2d, e, f show the lattice fringes at the tip A of the main trunk and at the tips B and C of the secondary branches on the left and right sides of the main trunk, respectively. The lattice spacing of 0.22 nm between adjacent planes in each of these images corresponds to the distance between two (100) crystal planes. Figs.2g~I show the SAED patterns of three areas A, B, and C of an individual petal and Fig.2J exhibits the ED pattern recorded from the whole petal. The SAED patterns recorded from different areas of the individual petal are almost identical. Zone axis projection is along [001]. The main trunk and secondary trunks on both side of the main trunk of the petal have equivalent growth directions: such as the main trunk oriented along [110] with the two branches along $[2\bar{1}0]$ and $[\bar{1}20]$[33]. HRTEM image and the sharp diffraction spots show that cobalt flower composed of nanoparticles seems to be the single-crystalline. It may be deduced that the nanoparticles constituted Co flower are aligned in a common crystallographic axis, which, therefore, exhibits scattering property similar to a single crystal. It is the character of the mesocrystalline.

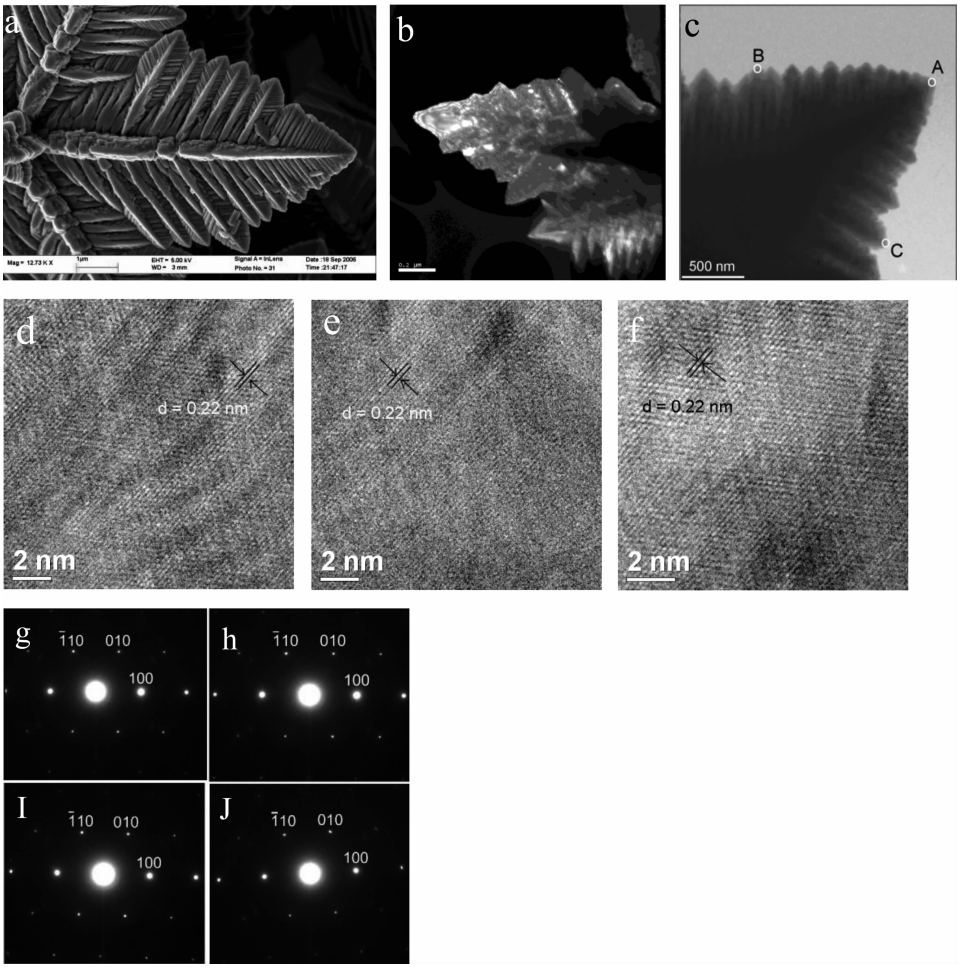

Fig.2 (a) FESEM image of a Co petal, (b) Dark field TEM image of a Co petal, (c) TEM image of a Co petal [mark A: the tip of the main trunk; B: the tip of left secondary branch; C: tip of right secondary branch], (d, e, f) HRTEM images recorded from the A, B, C respectively in Fig.2c. (g, h, I) SAED patterns recorded from A, B, C of Fig.2c respectively, (J) ED patterns recorded from a petal of Co flower

2.2 SEM and TEM characterization of the sample obtained under different experimental conditions

The influence factors on the formation of mesocrystal include surfactants, particles formation rate and reaction medium etc. As we learn from equation (**1**),

$$N_2+4H_2O+4e=N_2H_4+4OH^-,$$

$$\varphi^{\ominus}_{N_2/N_2H_4}=-1.15\ V \qquad (\mathbf{1})$$

the reducibility of N_2H_4 depends on the concentration of OH^- and N_2H_4. That is, the NH_2NH_2 reductibility increases with concentration of alkaline and NH_2NH_2 increasing, therefore the reduction rate of Co^{2+} to Co^0 increases significantly, which directly leads to the increase in the nucleation and formation rate of cobalt and is beneficial to form cobalt flower by nanoparticle mediated mechanism. Figs.3a,b show the SEM images of the sample reacted for 360 min at 0.25 mol·L^{-1} and 0.75 mol·L^{-1} of NaOH concentration, respectively, while keeping the other parameters constant. At a lower NaOH concentration, the irregular spherical aggregates of Co^{2+} nanoparticles are formed (Fig.3a) and the diameter of the spheres decreases with the reduction rate of Co^{2+} increasing (Fig.3b). At a lower concentration of NaOH, Co formation rate is slower. It is beneficial to aggregate into larger spheres. When increasing the concentration of NaOH, Co^{2+} reduction rate increases, leading to an increase in the nucleation rate of Co, therefore, the diameter of cobalt microsphere decreases. When the concentration of

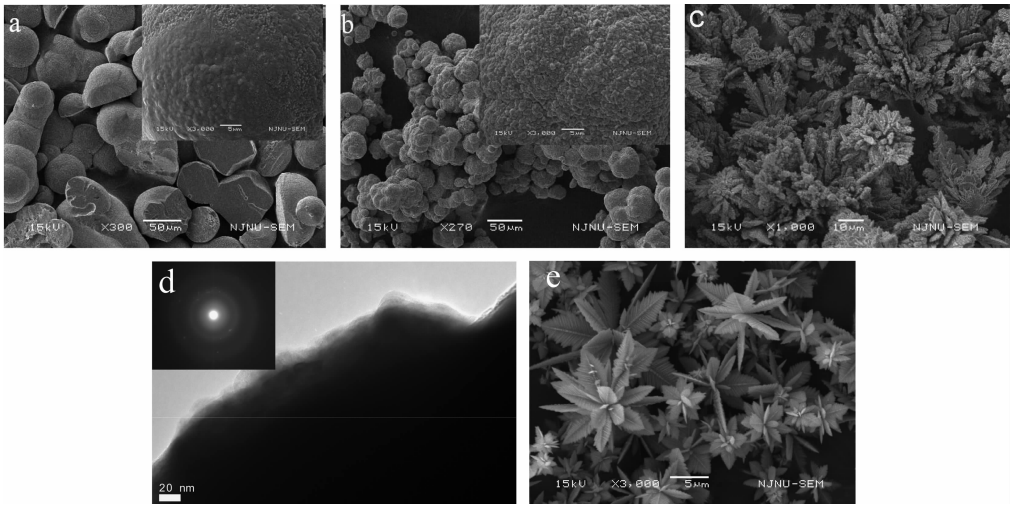

Fig.3　SEM images of the products obtained under a various concentrations of NaOH and reaction times in the hydrothermal system composed of DETA (7.5 mL), $CoCl_2$ (1.429 mol·L^{-1}) and $N_2H_4·H_2O$ (5 mL): (a) 0.25 mol·L^{-1} for 360 min; (b) 0.75 mol·L^{-1} for 360 min; (c) 1.25 mol·L^{-1} for 20 min; (d) TEM image of the products obtained at NaOH (1.25 mol·L^{-1}) for 20 min (ED pattern insetting); (e) 3.75 mol·L^{-1} for 10 min

NaOH increases to 1.25 mol·L^{-1}, the formation rate of cobalt farther increases, which is of benefit for 1D growth to form the dendrites-like structures composed of Co nanoparticles (Fig.3c). Fig. 3d and inset show the corresponding TEM image and ED pattern. The diffraction circles in the ED pattern clearly indicate that the dendrites are polycrystalline. Further increasing the concentration of NaOH, the well-defined flower-like structures(Fig.3e) are formed after reaction for 10 min. It is reasonable that when the NaOH concentration is high enough, the cobalt formed explosively, therefore, there have enough cobalt for simultaneous growth of main trunk, second and third generation trunk to form nice cobalt flower-like structure. Similar results are obtained by increasing $N_2H_4·H_2O$ amount. Figs.4a~d and SI~3 show the evolution of the shape for the products with $N_2H_4·H_2O$ amount increasing, from poor-look branch structure to the exquisite

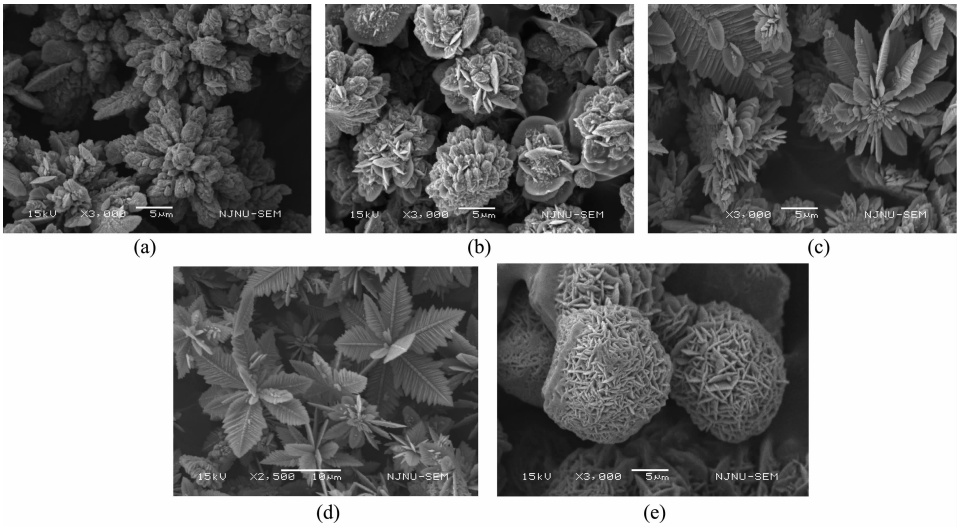

Fig.4　SEM images of the products obtained under various amounts of $N_2H_4·H_2O$ and reaction times in the hydrothermal system of DETA (7.5 mL), $CoCl_2$ (1.429 mol·L^{-1}) and NaOH (5 mol·L^{-1}): (a), (b) 0.3 mL and 0.5 mL respectively for 3 h; (c), (d) 3 mL and 5 mL respectively for 10 min, (e) SEM images of the products obtained at typically synthesis condition except using 40 ℃ instead of 100 ℃ for 12 h

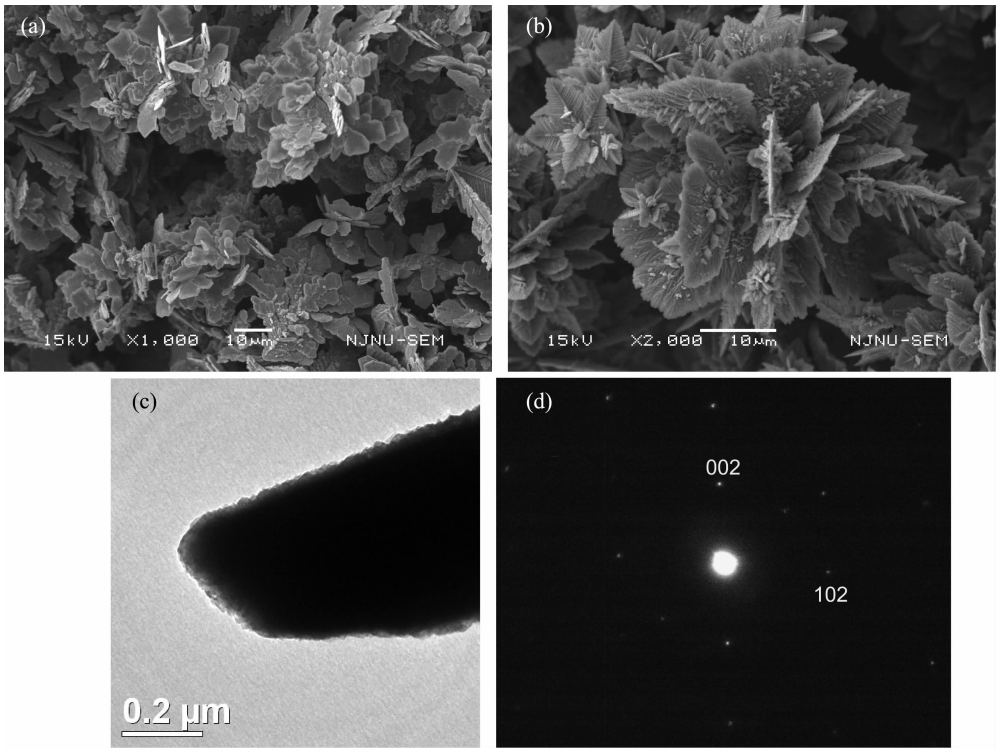

Fig.5 SEM images of the products obtained at various concentrations of DETA: (a) 0 mL, (b) 0.5 mL for 10 min at 100 ℃; Other reaction parameters were as follows: $CoCl_2$ (1.429 mol·L^{-1}), NaOH (5 mol·L^{-1}) and $N_2H_4·H_2O$ (5 mL), (c) TEM image of the Co plate obtained without DETA, (d) ED patterns recorded from a plate of Co flower

flower-like structure. The temperature significantly influences reaction rate of the system, and therefore the morphology of the products. Fig.4e displays that the shape of the products obtained at 40 ℃ is sphere composed of nanoplates. When temperature is very low, reaction rate is very low, which is beneficial to form spherical structure. The above results show that the cobalt morphologies can be well controlled by kinetic parameters such as reaction rate.

Influence of DETA on the morphology is shown in Fig.5. The perfect flower-like superstructures are formed by adding 7.5 mL of DETA (Fig.5a). Decreasing the amount of DETA to 0.5 mL and to 0 mL, the morphology of the superstructures becomes poor-look (Figs.5a,b). Fig.5a shows that Co flowers obtained without DETA are composed of several plates. Fig.5c shows TEM image of the plates, which are composed of nanoparticles. Corresponding ED pattern displays clear spots, which indicates that the plates are mesocrystals. At present time, we do not know the exact role played by DETA, but it might be related to the coordination interaction with as-formed cobalt nanoparticles.

2.3 Growth mechanism of Co mesocrystal

In order to further understand the formation mechanism of Co mesocrystal, control experiments are carried out under atmosphere and 100 ℃, which is convenient to observe the reaction progress with time. After the reaction bottle containing reactants is put into the oil bath and heated at 100 ℃ for 3 min, the formation rate of Co is quite slow, only very few black solid floated on the surface of solution. SEM image in Fig. 6a shows that the morphology of product is poor dendrite composed of Co nanoparticles and no flower-like Co mesocrystals are observed. After heated for 6 min, the reaction rate increases rapidly, a few flower-like Co mesocrystals appear (Fig.6b). After that time, the color of the solution becomes very violet and the reaction completes in 10 min. The flower-like Co mesocrystals are formed in large scale (Fig.6c). It provides further evidences for the above discussion. Taking a closer observation on SEM image of the

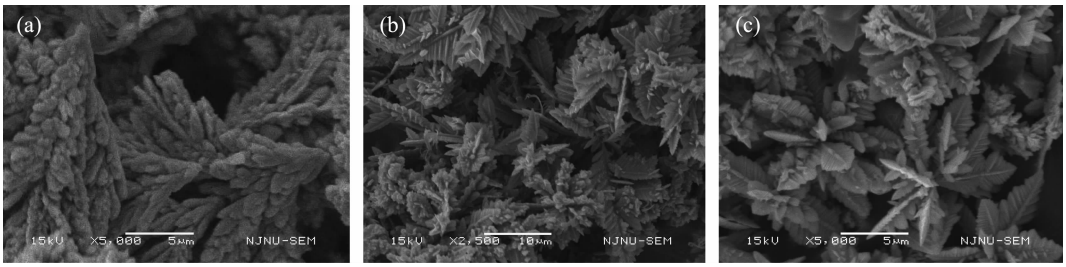

Fig.6 SEM images of the products obtained at the different time: (a) 3 min, (b) 6 min, c) 10 min under atmospheric pressure and 100 ℃, keeping other experimental parameters constant (DETA (7.5 mL), $CoCl_2$ (1.429 mol·L^{-1}), NaOH (5 mol·L^{-1}), $N_2H_4·H_2O$ (5 mL))

product, we can find a few of snowflake microstructure and the main product with 3D flower-like microstructure. For the snowflake microstructure, the seed is a hexagonal nanoplate and the 1D fast growth along the six crystallographic equivalent {100} directions of the hexagonal seeds occurs simultaneously in oriented-attachment fashion to form a sixfold-symmetric "snowflake". As we can see from Fig.1c that there have some protruding composed of Co nanoparticles in the center of the snowflake due to the nanoparticle oriented-attachment. The fast growth of 1D on those facets takes place simultaneously in oriented-attachment fashion when the reduction rate of Co^{2+} is high enough and cobalt atom is formed explosively, and then the flower-like mesocrystal forms. Flower-like Co mesocrystal are obtained using ethylenediamine (EN) instead of DETA while keeping the other experimental parameters constant (see SEM image of Co in the SI-4).

2.4 Magnetic properties

The magnetic properties of the cobalt mesocrystals were measured. From *M-H* curves in Fig. 7, the coercivity (H_c), saturation magnetization (M_s), and remanent magnetization (M_r) are obtained as *ca.* 401.3 Oe, 154.6 emu·g^{-1}, and 11.8 emu·g^{-1}, respectively, at 1.8 K and *ca.* 260 Oe, 153 emu·g^{-1}, and 12 emu·g^{-1}, respectively, at 300 K. The saturation magnetization is comparable to the bulk value (168 emu·g^{-1}) due to the micrometer scale (2~8 μm) of the Co flower mesocrystals[28,34], but it exhibits enhanced coercive force. Hc value of the bulk Co (a few tens Oe) is due to that Co flower mesocrystals are composed of smaller nanoparticles. It indicates that the Co flower mesocrystallines have not only properties of bulk Co but also the properties from the nanocrystals. Zero-field-cooling (ZFC) and field-cooling (FC) curves (575 K~750 K) for the Co mesocrystals in SI-5 exhibit that the ferromagnetic transition temperature T_c is higher than 750 K, which is beyond the measuring range of the magnetometer in our laboratory.

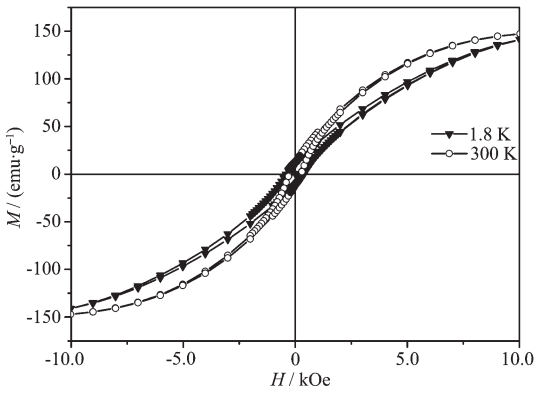

Fig.7 Magnetic hysteresis loops of as-prepared cobalt mesocrystals at 1.8 K and 300 K respectively

3 Conclusions

In summary, we have developed a facile and effective method for fabricating the well-defined cobalt flower-like mesocrystal in large scale and very short time(only 10 min). The cobalt flower-like mesocrystals exhibit the electron diffraction character of single crystals. The shape of Co superstructure can be adjusted by kinetic parameters. The saturation magnetization of the Co flower-like superstructure is comparable to the bulk cobalt metal because of the large size (2~8 μm), while the coercive force is higher than that of bulk metal due to properties from the nanocrystals. The exquisite structure is beneficial to

fundamental research for the formation mechanism of the mesocrystals and potential application in the field of catalysis, high-density data storage and sensor etc.

Supporting information is available at http://www.wjhxxb.cn/wjhxxbcn/ch/index.aspx.

References:

[1] Ma M G, Cölfen H. *Curr. Opin. Colliod Interface Sci.*, **2014**, **19**:56-65

[2] Cölfen H, Antonietti M. *Angew. Chem. Int. Ed.*, **2005**,**44**: 5576-5591

[3] Meldrum F C, Cölfen H. *Chem. Rev.*, **2008**,**108**:4332-4432

[4] Zhou L, O′Brien P. *Small*, **2008**,**4**:1566-1574

[5] Zhou L, Smyth-Boyle D, O′Brien P. *J. Am. Chem. Soc.*, **2008**, **130**:1309-1320

[6] Li T, You H J, Xu M W, et al. *Appl. Mater. Interfaces*, **2012**, **4**:6942-6948

[7] (a)Oaki Y, Imai H. *Small*, **2006**,**2**:66-70
(b)Popovic J, Cakan R D, Tornow J, et al. *Small*, **2011**,**7**:1127-1135

[8] Yao R M, Cao C B, Bai J. *CrystEngComm*, **2013**,**15**:3279-3283

[9] Ye J F, Liu W, Cai J G, et al. *J. Am. Chem. Soc.*, **2011**,**133**: 933-940

[10]Mo M S, Lim S H, Mai Y W, et al. *Adv. Mater.*, **2008**,**20**: 339-342

[11](a)Li Z H, Gener André, Richters J P, et al. *Adv. Mater.*, **2008**,**20**:1279-1285
(b)Wang S S, Xu A W. *CrystEngComm*, **2013**,**15**:376-381
(c)Liu Z, Wen X D, Wu X L, et al. *J. Am. Chem. Soc.*, **2009**, **131**:9405-9412

[12]Zhou N, Uchaker E, Wang H Y, et al. *RSC Adv.*, **2013**,**3**: 19366-19374

[13]Sun J X, Chen G, Pei J, et al. *J. Mater. Chem.*, **2012**,**22**: 5609-5614

[14](a)Tachikawa T, Zhang P, Bian Z F, et al. *J. Mater. Chem. A*, **2014**,**2**:3381-3388
(b)Thachepan S, Li M, Mann S. *Nanoscale*, **2010**,**2**:2400-2405

[15]Jongen N, Bowen P, Lemaitre J, et al. *J. Colloid Interface Sci.*, **2000**,**226**:189-198

[16]Johannes I, Bots P, Kulak A, et al. *Adv. Funct. Mater.*, **2013**,**23**:1965-1973

[17]Yuwono V M, Burrows N D, Soltis J A, et al. *J. Am. Chem. Soc.*, **2010**,**132**:2163-2165

[18]Zhou Y, Wang X Y, Wang H, et al. *Dalton Trans.*, **2014**,**43**: 4711-4719

[19]Dang F, Hoshino T, Oaki Y Y, et al. *Nanoscale*, **2013**,**5**: 2352-2357

[20]Song R Q, Xu A W, Antonietti M, et al. *Angew. Chem. Int. Ed.*, **2009**,**48**:395-399

[21]Liu Y Q, Kumar A, Fan Z, et al. *Appl. Phys. Lett.*, **2013**, **102**:232903(1-5)

[22](a)Fang J X, Ding B J, Song X P. *Appl. Phys. Let.*, **2007**,**91**: 083108(1-3)
(b)Fang J X, Ding B J, Song X P, et al. *Appl. Phys. Lett.*, **2008**,**92**:173120(1-3)
(c)Fang J X, Ding B J, Song X P. *Cryst. Grow. Des.*, **2008**,**8**: 3617-3622

[23]Fang Z, Long L Y, Hao S H, et al. *CrystEngComm*, **2014**, **16**:2061-2069

[24](a)Guo X H, Yu S H. *Cryst. Grow. Des.*, **2007**,**7**:354-359
(b)Guan M Y, Zhu G X, Shang T M, et al. *CrystEngComm*, **2012**,**14**,6540-6547

[25](a)Wang M S, Zhang Y P, Zhou Y J, et al. *CrystEngComm*, **2013**,**15**:754-763
(b)Park N H, Wang Y F, Seo W S, et al. *CrystEngComm*, **2013**,**15**:679-685

[26]Puntes V F, Krishnan K M, Alivisatos A P. *Science*, **2001**, **291**:2115-2117

[27]Xiemuxiding Abula(谢木西丁·阿布拉), Beysen Sadeh(拜山·沙德克), Mutila Aman(木提拉·阿曼), et al. *Chinese J. Inorg. Chem.*(无机化学学报), **2012**,**28**(7):1403-1408

[28]HE Wen-Qi(贺文启), XIAO Yong(肖勇), CHENG Jia-Liang(成嘉亮), et al. *Chinese J. Inorg. Chem.*(无机化学学报), **2010**,**26**(9):1685-1689

[29]An K, Lee N, Park J, et al. *J. Am. Chem. Soc.*, **2006**,**128**: 9753-9760

[30]YANG Pei-Xia(杨培霞), AN Mao-Zhong(安茂忠), SU Cai-Na(苏彩娜), et al. *Chinese J. Inorg. Chem.*(无机化学学报), **2007**,**23**(9):1501-1504

[31]Liu X, Yi R, Wang Y, et al. *J. Phys. Chem. C*, **2007**,**111**: 163-167

[32]Zhu L P, Xiao H M, Zhang W D, et al. *Cryst. Growth Des.*, **2008**,**8**:1113-1118

[33]Cao M H, Liu T F, Gao S, et al. *Angew. Chem. Int. Ed.*, **2005**,**44**:4197-4201

[34]Bao J C, Tie C Y, Xu Z, et al. *Adv. Mater.*, **2002**,**14**:44-47